BESST: A Miniature, Modular Radiometer

Robert Warden*, William Good* and Erik Baldwin-Stevens*

Abstract

A new radiometer assembly has been developed that incorporates modular design principles in order to provide flexibility and versatility. The assembly, shown in Figure 1, is made up of six modules plus a central cubical frame. A small thermal imaging detector is used to determine the temperature of remote objects. To improve the accuracy of the temperature reading, frequent calibration is required. The detector must view known temperature targets before viewing the remote object. Calibration is achieved by using a motorized fold mirror to select the desired scene the detector views. The motor steps the fold mirror through several positions, which allows the detector to view the calibration targets or the remote object. The details, features, and benefits of the radiometer are described in this paper.

Introduction

The availability of small, low-cost infrared detectors has enabled the development of small, low-cost thermal imaging instruments. The radiometer, which is the subject of this paper, uses this technology to remotely detect the surface temperature of large bodies of water. Knowledge of the surface temperature of the ocean is an important factor in weather prediction. Currently, the temperature is recorded by large instruments onboard ocean going ships. These instruments are very accurate but are also large and heavy. The temperature readings are limited to the path of the ship so relatively few data points are available for weather forecasting models. Achieving the high accuracy desired requires frequent and regular calibration. This is challenging for the instrument design and usually requires increased volume, mass, and complexity.

The Ball Experimental Sea Surface Temperature (BESST) radiometer was designed and built by Ball Aerospace as a small, modular, light-weight and low-power sensor for sea surface temperature (SST) studies from an Unmanned Aerial Vehicle (UAV). BESST has been demonstrated on a conventional Twin Otter airplane and is part of several NASA proposals. It incorporates a commercial detector to sense the infrared radiation from the surface of the water and features two on-board calibration targets in addition to the ability to view the sky for background readings. BESST uses a combination of windows and filters to improve accuracy by minimizing the effect of water vapor and aerosols in the atmosphere. Special absorptive or reflective paints and treatments are used on the various surfaces, as needed. The resulting measurements of the absolute sea surface temperature are accurate to within 0.3°C.

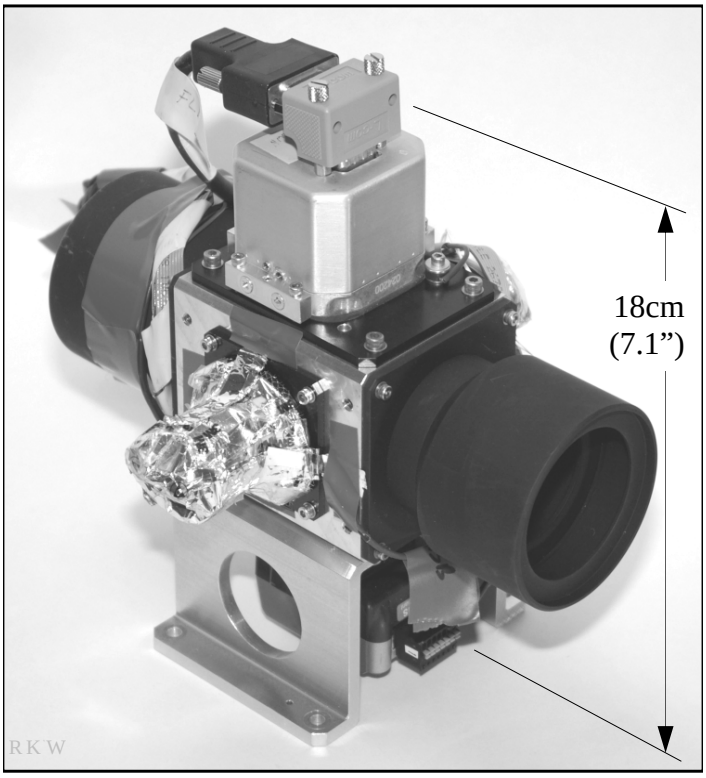

Figure 1. BESST Radiometer

* Ball Aerospace & Technologies, Boulder, CO

Background

Accurate readings of Sea Surface Temperature (SST) are crucial to modeling water-energy cycles, which are used for weather prediction and understanding climate change. Satellite measurements cover broad areas but must be calibrated with actual surface measurements of the water temperature. Current NASA satellites such as the Moderate Resolution Imaging Spectroradiometer (MODIS) and Advanced Very High Resolution Radiometer (AVHRR) operated by NOAA, provide SST measurements with a spatial resolution of one kilometer and a precision of 0.1°C. These satellite SST sensors are calibrated with ship-borne SST instruments that provide a few single point measurements. The ship-board instruments are very expensive to build, operate, and deploy.

The BESST modular radiometer offers an alternative for calibration and validation of on-orbit SST instruments. This alternative uses a small, lightweight radiometer integrated to an Unmanned Aerial Vehicle or conventional aircraft to provide highly accurate, high-resolution SST data for frequent, lower-cost validation of satellite data. The BESST radiometer system has a precision of 0.1°C and can be flown quickly over a large area providing a more complete calibration/validation of image data from the orbiting satellite than is available from ship-borne instruments.

In addition to calibration and validation of satellite measurements, the BESST radiometer can perform studies not previously possible with current SST instruments. BESST can perform high spatial resolution mapping of single satellite pixels to look for small-scale variability in infrared SST patterns. This is particularly important near coastal areas and where rivers empty into coastal waters and form estuaries critical to near-shore activities. Understanding small-scale variability will provide insight and may help close the air-sea heat budget. Figure 2 shows the small-scale variability present within satellite pixel data. Data from the MODIS satellite, large square pixels, is shown with 2 strips of data from a BESST airborne measurement overlaid. The BESST plot clearly shows temperature variability within that region that can significantly affect ocean and climate models.

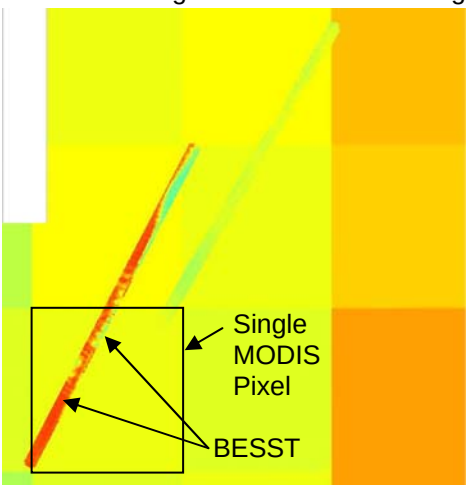

Figure 2: BESST data showing fine structure within MODIS single pixels

Another possible application for the BESST radiometer is the study of diurnal warming. Variability of SST on sub-day time scales is often dominated by the diurnal solar warm layer phenomenon. This warm layer is stronger in lighter winds and solar forcing. In light winds (<2 m/s) it can exceed 2 percent. The depth is inversely proportional to the strength.

There are a number of ways to account for the warm layer in relating SST to the actual subsurface temperature structure. Fairall et al. (1996a) present a simple 1-D model integrated into the COARE bulk flux model (Fairall et al., 1996b, 2003). More recently, Zeng and Beljaars (2005) developed a similar scheme that has been implemented at European Centre for Medium-Range Weather Forecasts (ECMWF) (Brunke et al., 2008). The Fairall scheme was developed and optimized for tropical applications and does not include physics to deal with turning of the near-surface currents by the Coriolis force. Thus, the timing and magnitude of this warm layer at mid-latitudes may not be well-described by the model.

To date, studies of diurnal warming in the SST measurements have been limited to multi-day measurements indicating amplitude change over time. The BESST radiometer can be deployed over a region for full 2D spatial mapping of the diurnal signal at a specific time making it a unique tool for the SST community. Diurnal warming has been recently identified by a NASA study group on SST as the primary uncertainty in satellite SST measurements, and this unique capability of the BESST to study this

temporal/spatial variability greatly increases its importance in being able to augment the ship-based surface temperature measurements.

Design Development

The accuracy of the temperature reading relies on frequent calibration, which involves having the detector look at known temperature sources before looking at the remote object. The initial design requirement was very simple: place a black-body target in front of the optical path in order to calibrate the detector. The initial configuration was to have some sort of flip mechanism to move a black-body target in and out of the detector field of view. It was then determined that two calibration targets should be used: one for the warm black-body and another for ambient temperature. To accommodate two calibration sources, a three position flip mechanism was proposed.

The final design requirement was that a second scene select was needed to look at the sky. It was apparent that in order to get a second sky view, either the detector had to move or a fold mirror was needed to reflect the image through a second baffle tube. The development of the design is shown graphically in Figure 3. Note that each double-ended arrow represents a separate mechanism.

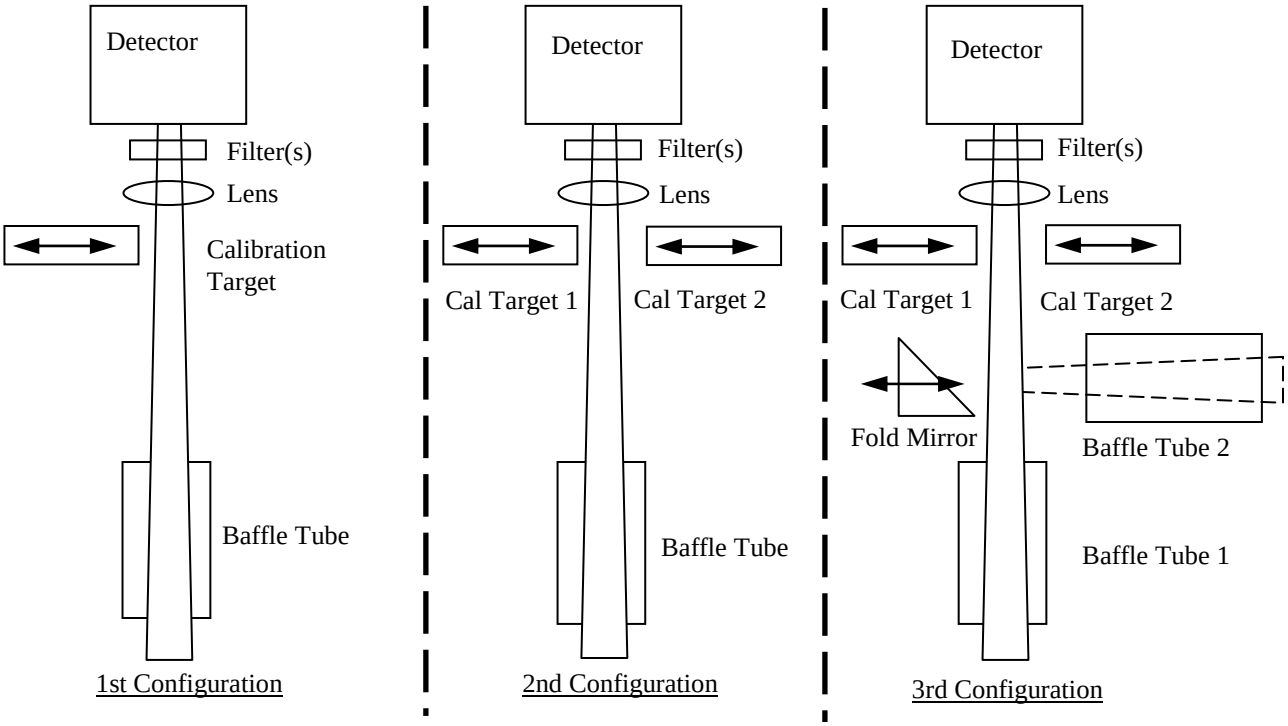

Figure 3. Design Iteration Showing Increasing Complexity

The key design breakthrough was realizing that if a fold mirror was acceptable for one scene, it could be acceptable for all scenes. By rotating the fold mirror as shown in Figure 4, the detector could easily be exposed to different scenes. It is also a benefit to have the fold mirror always in place so that the only variable is the scene.

The design iteration went as shown in Figure 3 with the development progressing at a sketch level before detailed design work was started. A set of well defined concepts and parameters were evaluated before the design work started. The final configuration is the best compromise between optics, thermal, cost and schedule.

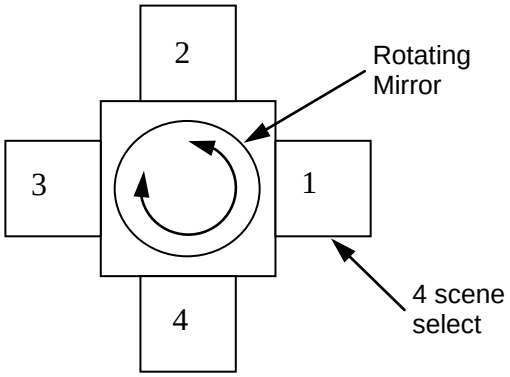

Figure 4. Final Single-Mechanism Configuration

Operation

The basic principal of the design is to have the motor/fold-mirror opposite the detector assembly as shown in Figures 5 and 6. The motor rotation axis is directly in-line with the center of the detector. In this way, the optical path reflects off the fold mirror and can be directed by rotating the fold mirror. The optical path always reflects off the mirror so that the only difference to the detector is the actual scene. In addition, the optical stop is built into the turret, so the stop rotates with the mirror.

On-board calibration is done by alternating the observed scene from the ocean and two temperature-monitored black-body references, the common "two-point" method in radiometers with one heated and the other at ambient instrument temperature. An absolute calibration of these reference blackbodies is performed in the laboratory prior to deployment. A third "sky" port is also available to measure sky radiance to extract its reflection from the ocean temperature measurement. The use of microbolometers eliminates the need for cryogenic fluids, greatly simplifying flight requirements.

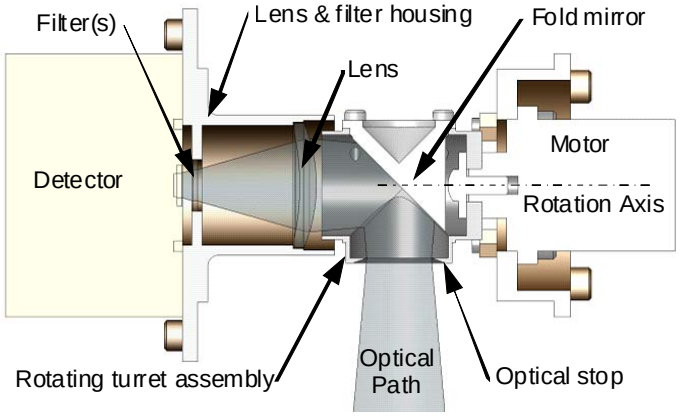

Figure 5. Detector, Mirror & Motor

For calibration, the mechanical design has three desirable features. First, the tight fit between the mirror housing and the lens housing keeps stray light off of the calibration sources. Second, the angle of incidence of the mirror is equal for the calibration sources and the scene. Third, the area of the mirror used is the same for both the calibration sources and the scene.

Description

The six modules that go into the assembly are shown in Figure 7. The central cubical frame is universally symmetric so that any module can mount to any face. The detector module is mounted opposite the motor module previously shown in Figure 5. The motor rotates to position the turret and fold mirror to one of four quadrants. These faces can accommodate either a calibration target or a baffle tube. Light (or heat) from any one of the four faces can then be directed to the detector. The calibration and baffle modules typically mounted on these faces are discussed later in the paper.

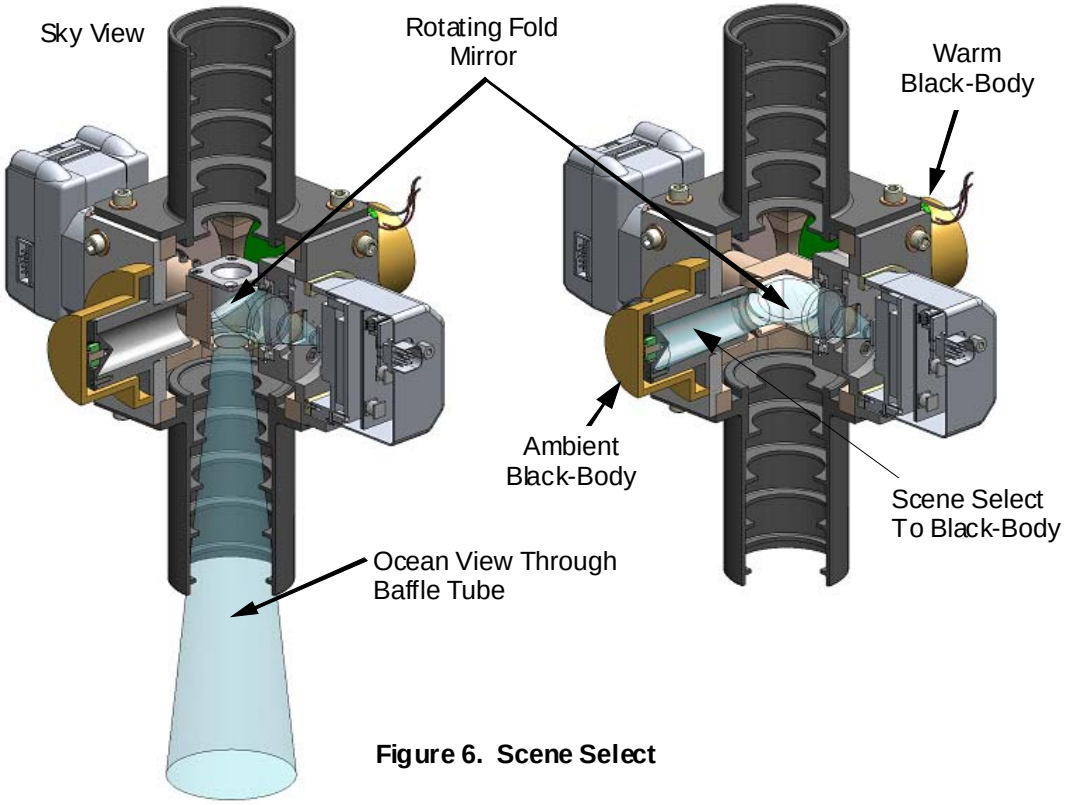

Figure 6. Scene Select

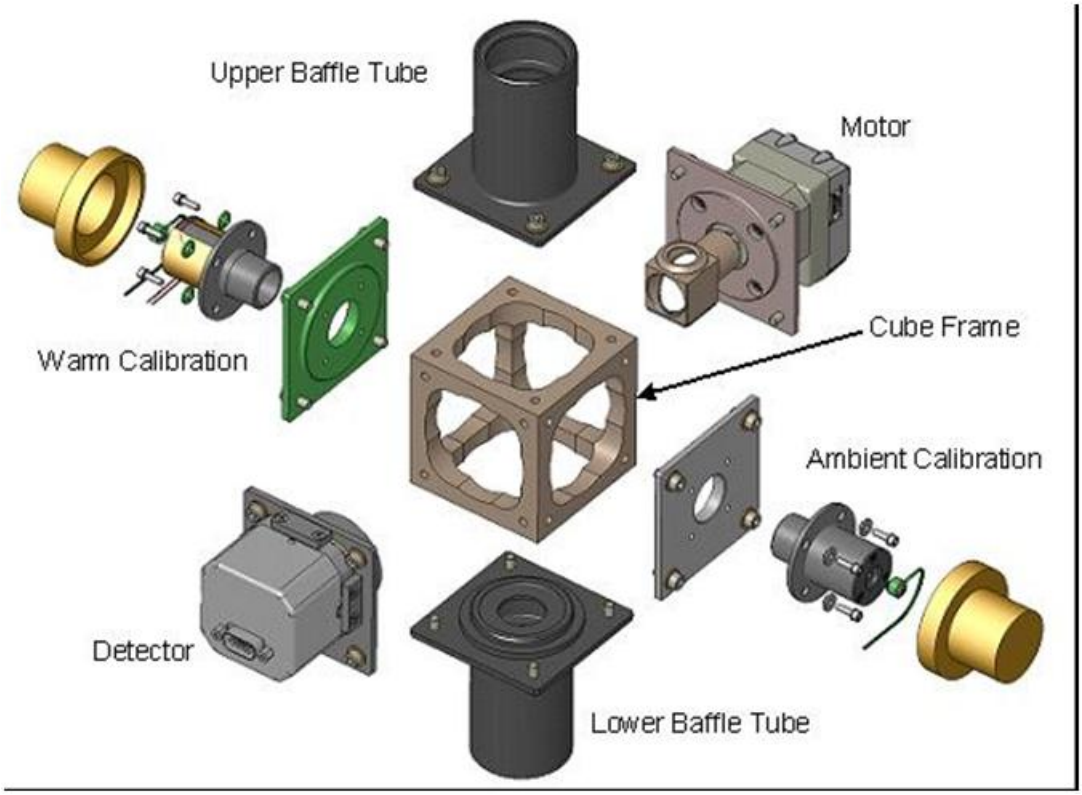

Figure 7. Modules & Frame

Mounting

The BESST instrument can be mounted on any of the six faces as shown in Figure 8 by using a custom bracket to interface with the airborne or terrestrial vehicle. The bracket can also provide additional thermal isolation from the vehicle. The lightest-weight option is to have the support vehicle provide a mounting interface.

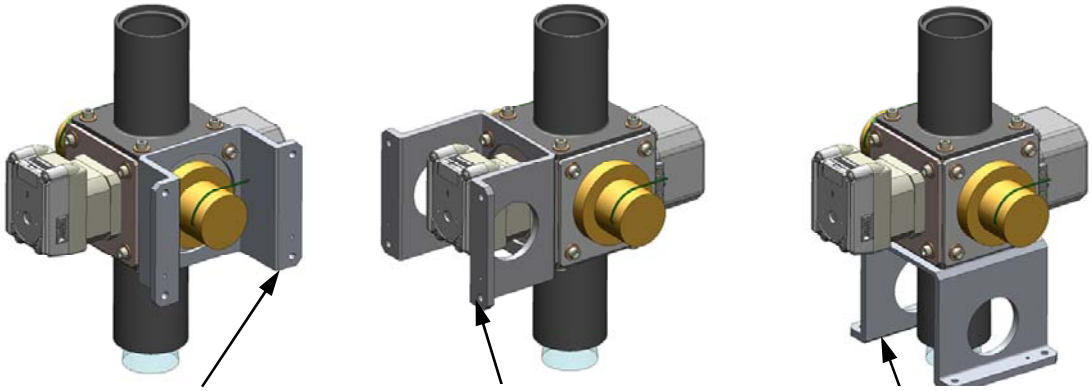

Figure 8. Mounting Options

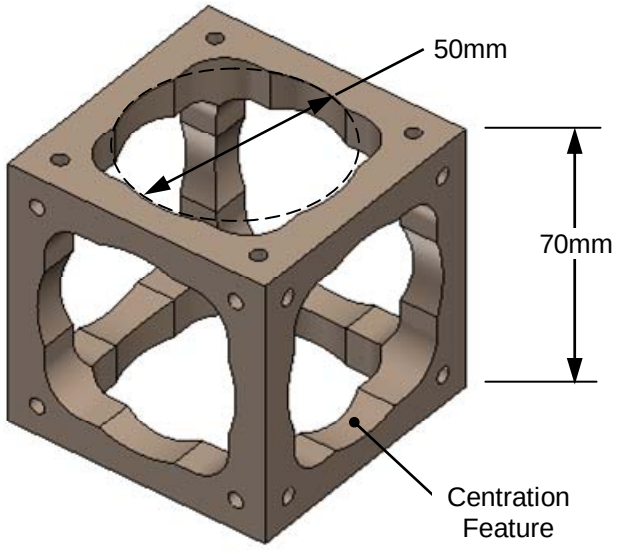

Figure 9. Cube Frame

Cubical Frame

The central structure or chassis for the assembly is a simple hollow cube as shown in Figure 9. Each side is 70-mm long and each face has four tapped holes with which to attach the modules. The six faces are machined out of a single piece of aluminum so that the cube is lightweight but structurally sound. The mass of the aluminum cube is only 180 grams. The cube could be scaled up to accommodate a larger optical path.

Each face also has a diametral centration feature in the form of a close tolerance bore. Each module has a corresponding lip that fits into the bore. As the modules are attached to a given face, they are automatically aligned to the center of the cube. Modules can be replaced or rearranged while maintaining alignment. The focal length is unaffected by rearranging the modules because the distance from the face to the center of the cube is the same for each location.

Detector Module

The detector module consists of the detector as well as any lenses or filters required for the desired operation (Figure 10). A single housing is used to position the optical components so that this module can be aligned and verified as a stand-alone unit. The detector module has a total mass of 225 grams of which the detector assembly is 125 grams.

Two different detectors have been mounted to the radiometer. The original detector was made by Raytheon and the second detector was made by FLIR. Both are un-cooled microbolometers with a 324 X 256 array with a pixel size of 38 microns.

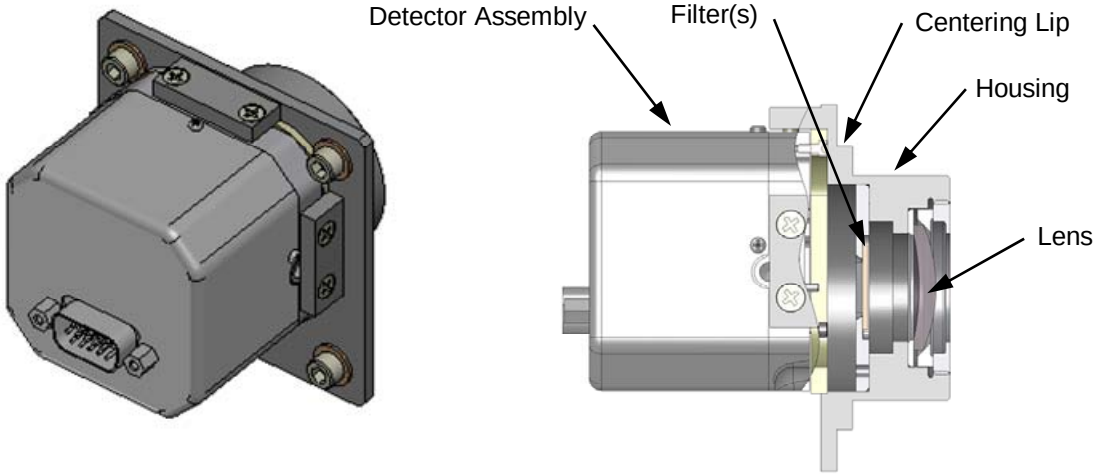

Figure 10. Detector Module

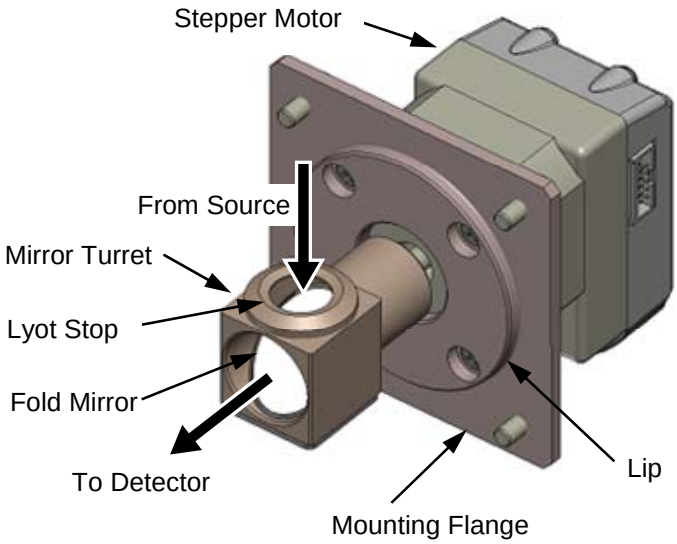

Figure 11. Drive Module

Motor Module

The key to the performance of the radiometer is the ability to easily calibrate the detector. This involves having the detector look at objects that have a known temperature in order to calibrate the output.

The motor module (Figure 11) supports a 45-degree fold mirror that directs the source of light to the detector. The fold mirror is mounted in a rotating turret and the entrance to the turret is the Lyot stop for the optical path.

The only load on the motor is from the turret and fold mirror, which are cantilevered off of the output shaft of the motor. The total offset load is only 33 grams. The total mass for the entire motor module is 380 grams; however, this includes a gearhead and control electronics.

Figure 12. MDrive 17 Motor and controller (300 grams)

Motor Details

The MDrive 17 motor/controller was selected for this program because it is a readily available commercial unit that comes with an integrated controller. At 300 grams, it is reasonably light-weight and the long shaft was convenient for attaching the turret and fold mirror. The unit also comes with a canned software package that loads easily onto a computer. Simple commands can be issued to rotate the mirror to the required quadrant. If step counts are lost, the unit can be commanded to find its home position in order to reset the zero degree location.

An even lighter-weight motor was desired to further reduce the weight of the system. When Sanyo Denki announced a new line of pancake stepper motors that are only 11-mm thick, the program purchased both the 42-mm version and the 50-mm version, as shown in Table 1. Although the new motors were very small and light, the output shaft was found to be too short. A longer version of the 42-mm motor is available with a longer shaft but it is the same weight as the original unit.

Table 2. Alternate motors considered

			
42mm pancake motor (70 grams)	42mm cube motor (240 grams)	50 mm pancake motor (90 grams)	MForce Controller (74 grams)

Overall mass and complexity could be reduced by using a simple 4-position motor; however, a commercial unit does not currently exist. The ideal motor would be a 90° stepper motor that could be rotated 90° with a single switch command. A detent at each quadrant position might be needed to assure repeatability if the natural cogging of the motor is not accurate enough.

Baffle Module

The baffle tube is constructed from a single piece as shown in Figure 13. The purpose of the baffle is to reduce the amount of stray light getting to the detector for the Earth and sky view scenes. The inside of the baffle is painted with a black absorptive paint. Baffle fins are placed so that undesired light is directed to the black surface after one bounce. The total mass for each baffle is 110 grams.

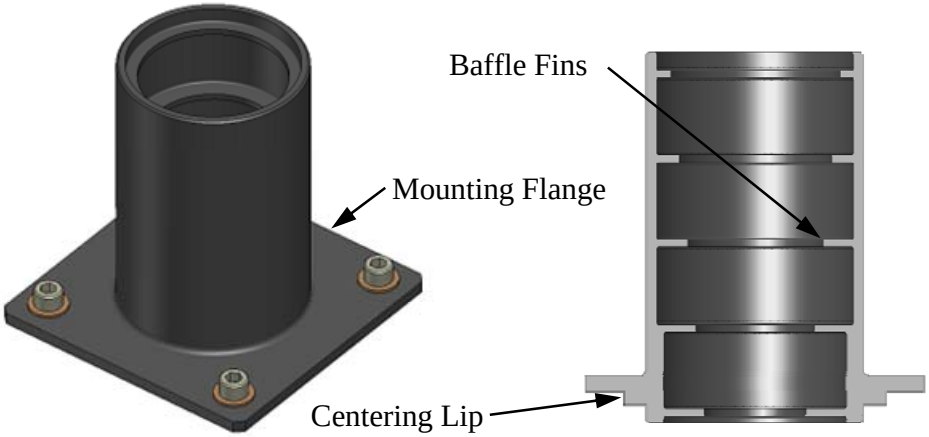

Figure 13. One Piece Baffle Tube

Calibration Module

The calibration target consists of an aluminum tube with a conical end that forms a black-body calibration source. The inside is painted with a black absorptive paint so that when the detector views the target, it sees an accurately defined and uniform temperature. The Calibration Module shown in Figure 14 can be built up in one of two configurations depending on the calibration temperature required. For warm calibration, a fiberglass mounting flange is used so that the black-body target is thermally isolated from the rest of the system. A strip heater, attached to the outside of the aluminum tube, heats the tube to a predefined temperature and a temperature sensor reports the temperature.

Using an aluminum mounting flange and no external heater, the temperature of the target is the same as the temperature of the cube, detector and baffles. No heater is used but a temperature sensor is mounted to the black-body to report the temperature of the assembly. The black-body and temperature sensor are covered by a "hat" made up of Multi-Layer Insulation (MLI). The wires from the temperature sensor and strip heater exit through a small hole in the MLI cover. The mass of the calibration module with the fiberglass mounting flange is 95 grams and the module with the aluminum plate is 110 grams.

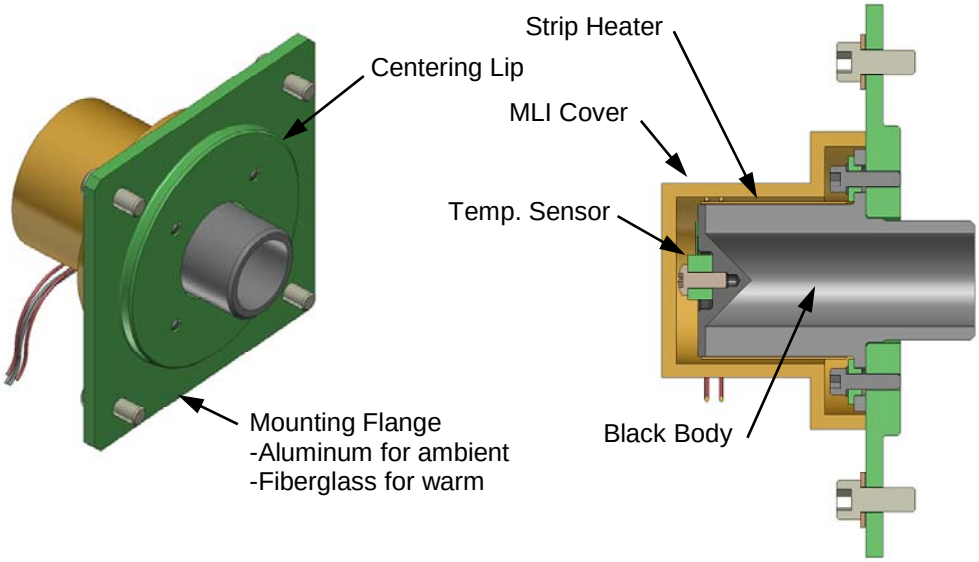

Figure 14. Calibration Modules

Mass

The total mass of the BESST instrument shown in Table 2 is for the radiometer and mechanism only and does not include the electrical cables, computer or battery required for the entire system. Reasonable dimensions and tolerances were used for this development unit. Additional mass savings could be achieved using more complicated machining.

Table 2. Mass Summary

Module	Mass (grams)
Cube Frame	180
Motor	380
Detector	225
Baffle	110
Baffle	110
Cal Source	95
Cal Source	110
Mounting Bracket	150
Total	1.36 kg (3 lb)

The heaviest component on the list is the motor. For this application, the motor also includes a gearhead and control electronics. A much simpler and lighter motor could be procured but the selected unit was inexpensive, easy to interface with and easy to control.

Alternate configurations

Several different configurations are possible as shown in Figure 15. Using the existing central cube, the baffle tubes and calibration targets can be moved around to accommodate the desired mission. The central cube can be replaced with a hexagonal housing to provide additional target viewing options.

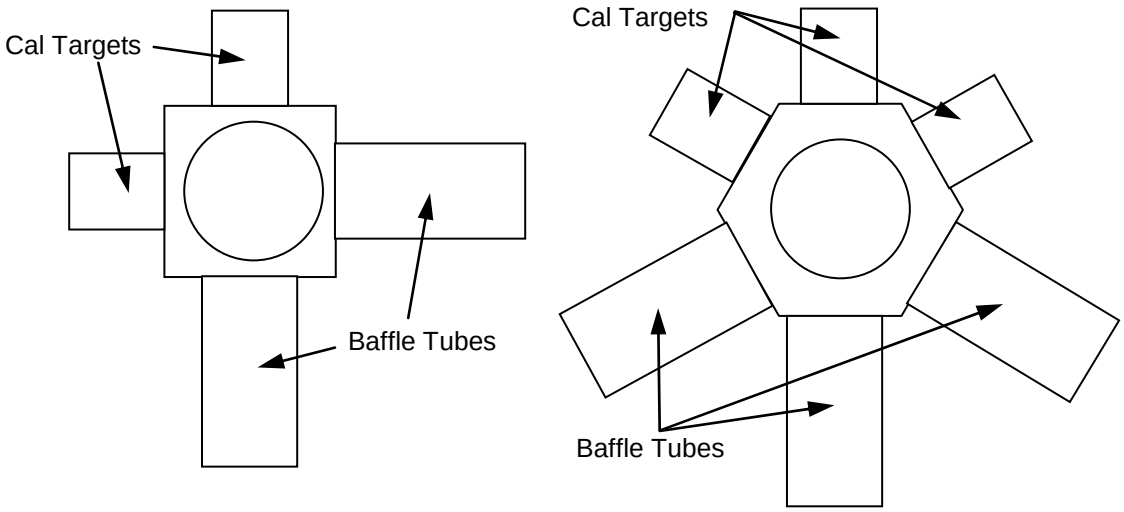

Figure 15. Alternate Configurations

The resulting assembly is a compact sensor approximately the size of a 20-cm cube as shown in Figure 16. Not included in this volume are the mounting brackets, electrical cables, computer and batteries. Also, extended baffle tubes may be needed for specific scene viewing.

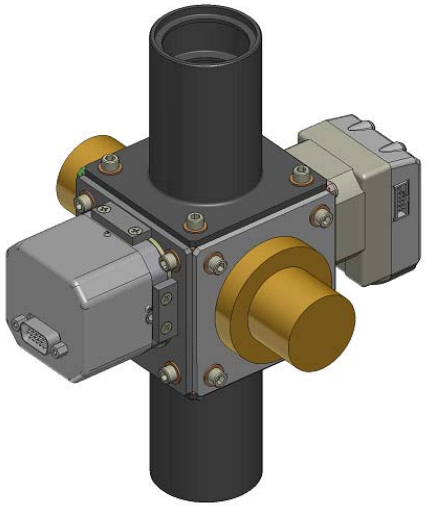

Figure 16. Overall assembly

Flight Performance

The first “flight” of the BESST instrument was actually a field test at a local Colorado lake. The instrument was cantilevered off the side of a small dock as shown in Figure 17. This test simulated the important parts of the system by having a view of the water as well as a view of the sky.

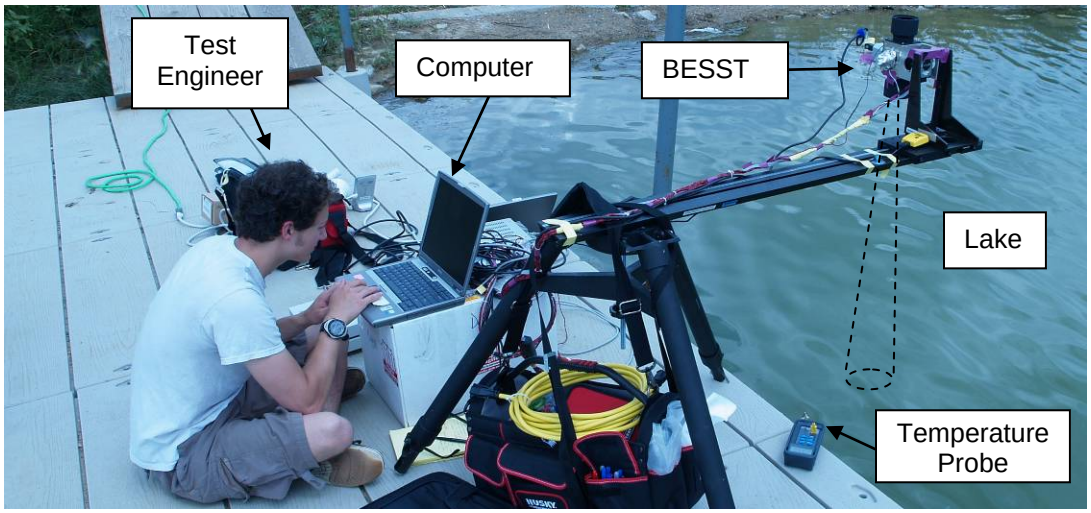

Figure 17. Field Testing

Electronics

The block diagram of the electronics for BESST is shown in Figure 18. The Airborne Computer commands the motor position and records the data from the detector. The motor is commanded to rotate the central fold mirror to view the four scenes: water, sky, warm black-body, and ambient black-body. The detector captures images of each scene through the sequence and the black-body readings are used to provide a highly accurate calibration of the scene measurement. The sequence is automated through the software to collect data over a region of interest.

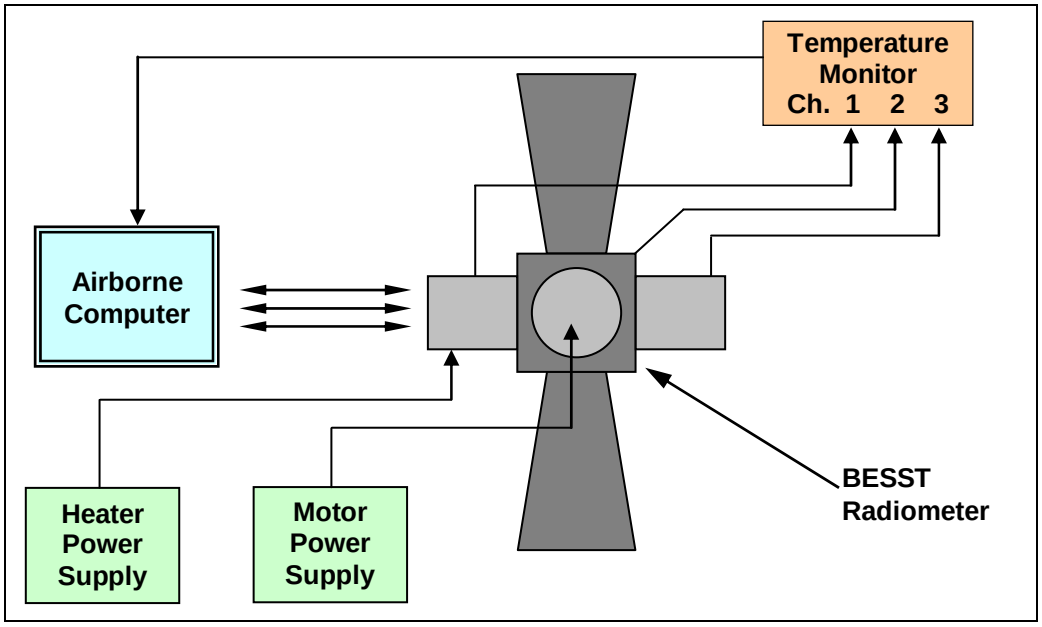

Figure 18: BESST electronics block diagram

Test Results

The BESST radiometer demonstrated excellent performance in a test flight over Salt Lake, Utah. Flying at low altitude, it provided some of the highest resolution water surface temperature measurements yet achieved, as shown in Figures 19 and 20. Each pixel represents roughly 10 meters. The resulting detail uncovers significant spatial variability, with 1 to 2°C warm and cold pools on the order of 50 to 100 meters across.

Predicted noise levels on the order of 0.1°C have been achieved, and the instrument is sensitive to water temperature changes on this level. While absolute accuracy of the measurements cannot be verified for the test flight over Salt Lake, lab testing with controlled, uniform blackbodies has shown the instrument to be accurate to better than 0.3°C. Repeated flight passes have an RMS variability of 0.1°C.

Additionally, the orbiting Moderate Resolution Imaging Spectroradiometer (MODIS) passed over Salt Lake on the day of the test flight, collecting 1-km-resolution surface temperature data. The newly developed radiometer compares well to MODIS, with an average resolved surface temperature difference of roughly 0.9°C.

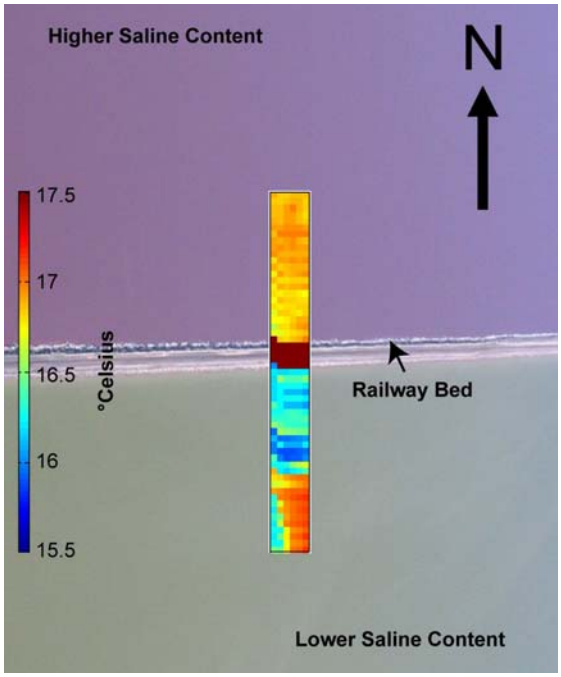

Figure 20. One data transect across a railroad with water on either side

Much of this difference may be attributed to the disparity in resolution between the radiometer and MODIS. Considering the small-scale surface temperature variation seen during the test flight and the small fraction of each MODIS pixel that was sampled (roughly 7%), this data is not expected to directly represent the average temperature over a 1-km^2 area measured by MODIS. The measurements match MODIS to within the level of spatial variation observed, confirming the accuracy of the instrument.

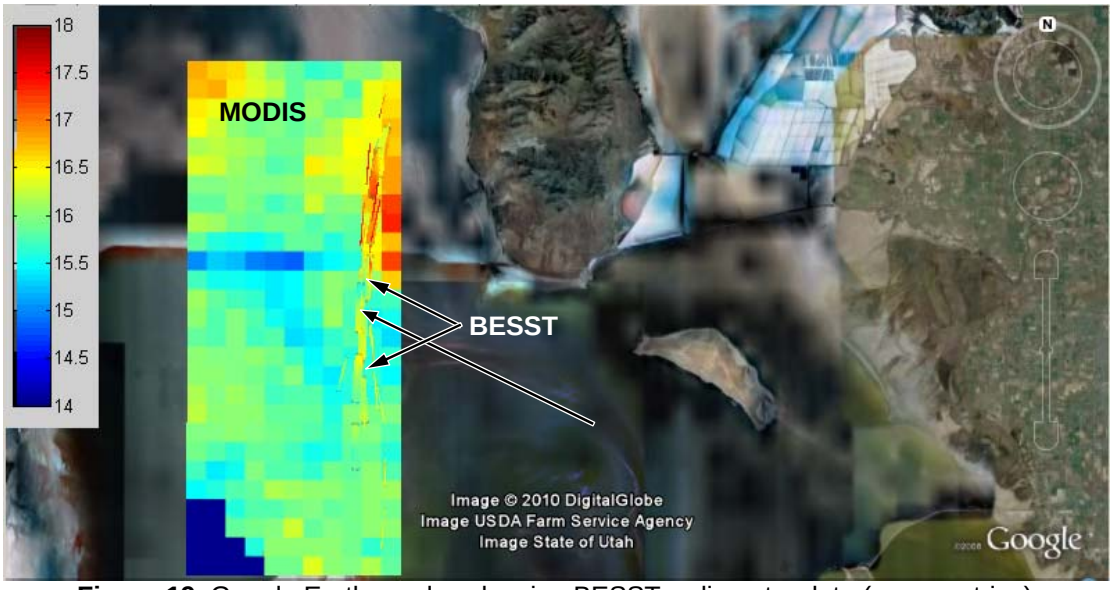

Figure 19. Google Earth overlay showing BESST radiometer data (narrow strips) and MODIS data (large pixels) over Salt Lake, Utah.

Applications

The Modular Radiometer can be used in several applications and environments. It was originally designed to fly on a UAV such as the Aerosonde shown in Figure 22. In this application, sea surface temperatures could be measured over long strips of ocean. The assembly is small and light enough to be compatible with this type of aircraft.

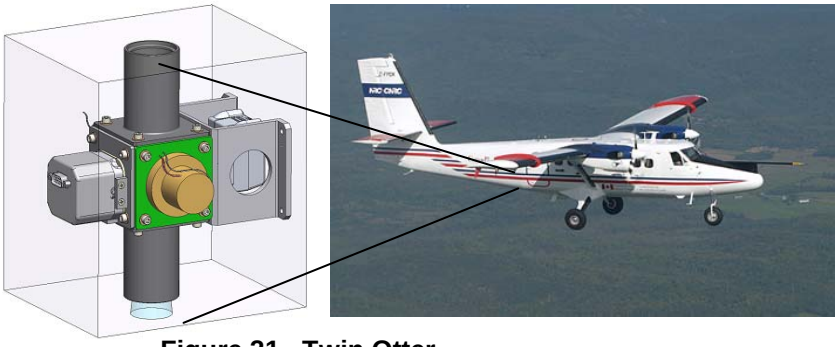

Figure 21. Twin Otter

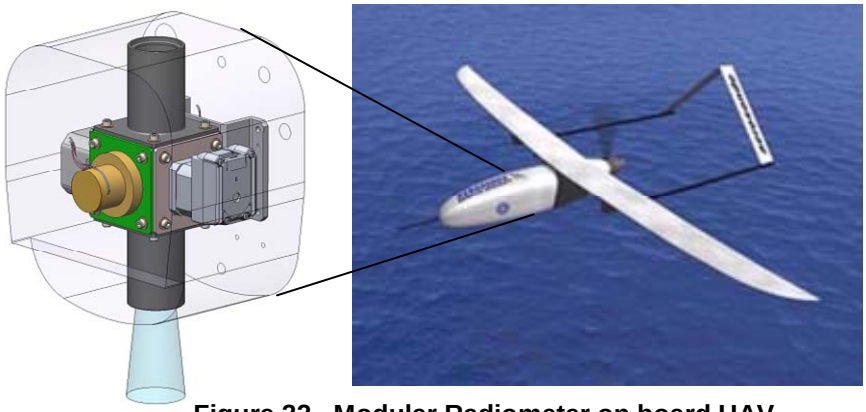

Figure 22. Modular Radiometer on board UAV

To demonstrate capability, however, it was re-configured with a different mounting bracket to fly on a Twin Otter, which is a plane commonly used to test prototype instruments (Figure 21). For this application, the unit was mounted to a central structure and controlled using a laptop computer. Aircraft inverters were available for power to the unit and computer.

With a space-qualified motor, detector and electronics, the Modular Radiometer could be mounted to a satellite to provide remote radiometric sensing capabilities (Figure 23).

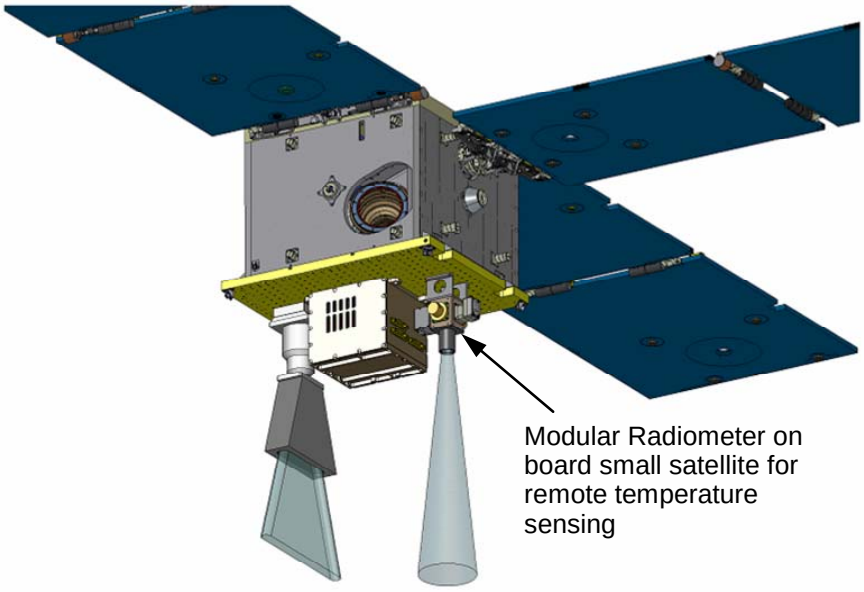

Figure 23. Mounted on Satellite

Lessons Learned

Much of the development of the BESST instrument went very well but there were some specific lessons that were learned that may be of use to the reader:

Communication

Always communicate the status and requirements of a program to all relevant disciplines. If the requirements are not known, make assumptions and communicate those assumptions to the team. For this program, mass was not an actual requirement other than to enable the instrument to be flown on a UAV or satellite at some later date. Consequently, a reasonable effort was made to make the parts light-weight. The mass of each component as well as the entire assembly was calculated regularly and distributed to the team members. Likewise, the voltage and current needed for the motor and heaters were also researched and reported. The systems engineers could then work with these values to anticipate any problems.

Documentation

Maintaining a centralized location for documenting changes to the design and layout of the system was crucial to the success of the instrument. In a development environment, the conceptual layout changes discussed herein impacted all areas of the system and needed to be well understood by each engineer on the project. Turnover of personnel during the lifetime of a project makes documentation even more important.

Detector

In the interest of making the cost per unit of the BESST instrument as low as possible while maintaining calibration accuracy, the original Raytheon Vision Systems bolometer was replaced with a FLIR bolometer which has a larger detector area. The initial unit was designed for the smaller Raytheon Vision Systems detector so that the initial baffle tubes were clipping the edges of the new light path. It was fairly easy to replace the original baffles with two new baffles tubes because of the modularity of the design as shown in Figure 24. The lesson learned is that it is advantageous to provide accommodations for potential detector upgrades or modifications.

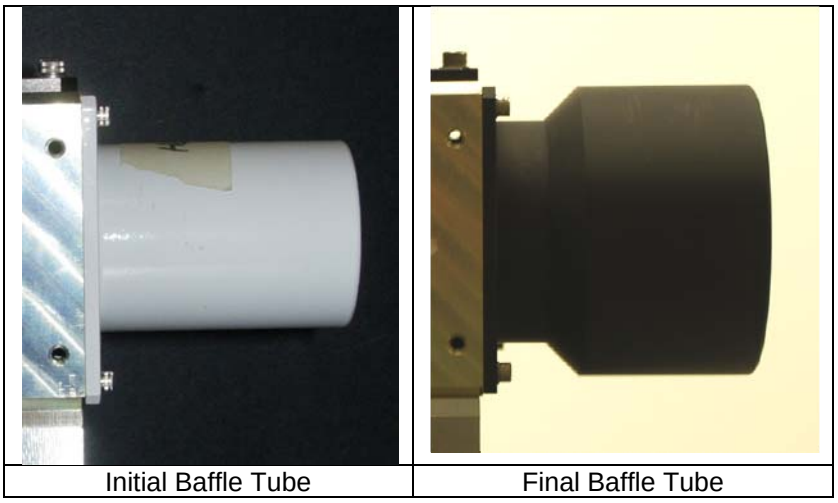

Initial Baffle Tube | Final Baffle Tube

Figure 24. Baffle Tubes

Motor

At the beginning of the program, it was envisioned that a small, simple motor could be procured that would rotate the fold mirror to the four positions. It was thought that a rotary solenoid or a four-pole motor could be used. A detent of some sort might be necessary to hold the mirror in position at the quadrant, but a command to move the motor 90 degrees should be very simple.

In practice, such a device could not be found. Motor vendors were willing to develop a custom motor for this program but the cost was too great for a development effort. The motor that was eventually used is compact and heavy although easy to command. The lesson learned from this is that a motor as a single design component can still be very complicated and difficult to obtain.

Conclusion

The radiometric performance of the BESST instrument meets the science requirements for SST studies for a much lower cost and with better spatial resolution. The accuracy of the microbolometer temperature readings are 0.09°C and the accuracy of the overall instrument is 0.3°C for individual pixels. The temperature accuracy and spatial resolution can be traded off: more pixels can be averaged to achieve better accuracy, but at the cost of lower spatial resolution. This is done during post-processing of the data and will be explored further as part of continued scientific demonstrations.

Laboratory and flight testing of the BESST radiometer have shown it to be a valuable complement to ship-borne SST instruments. In addition to performing calibration / validation activities for satellite SST sensors, BESST can perform measurements with higher spatial resolution and repeat area coverage than currently available instruments. The lightweight, modular design is responsible for these advantages as it allows the instrument to be deployed on a UAV platform in a configuration suitable to each mission.

Acknowledgements

The authors wish to acknowledge the help and support of Ray Demara, Paula Wamsley, Shelley Petroy and the Airborne Initiative group at Ball Aerospace. Also the hard work of numerous engineers, technicians and interns including Paul Kaptchen, Raymund To, Tony Lin and James Lasnik as well as Brian Johnson, Michele Kuester, Jennifer Turner-Valle, Kartik Ghorakavi and Julie Sandberg. A special thanks to Dr. William Emery of the University of Colorado for scientific guidance with respect to SST measurements and requirements.

References

Brunke, M.A., X.B. Zeng, V. Misra, and A. Beljaars, 2008: Integration of a prognostic sea surface skin temperature scheme into weather and climate models. J. Geophys. Res., 113, D21117.

Fairall, C.W., E.F. Bradley, D.P. Rogers, J.B. Edson, and G.S. Young, 1996: Bulk parameterization of air-sea fluxes for TOGA COARE. J. Geophys. Res., 101, 3747-3767.

Fairall, E.F. Bradley, J.S. Godfrey, J.B. Edson, G.S. Young, and G.A. Wick, 1996: Cool skin and warm layer effects on the sea surface temperature. J. Geophys. Res., 101, 1295-1308.

Fairall, C. W., E. F. Bradley, J. E. Hare, A. A. Grachev, and J. B. Edson, 2003: Bulk parameterization of air-sea fluxes: Updates and verification for the COARE algorithm. J. Clim., 16, 571-591.

Zeng, X.B., and A. Beljaars, 2005: A prognostic scheme of sea surface skin temperature for modeling and data assimilation. Geophys. Res. Lett., 32, L14605.